Damaging Long-period Ground Motions from the 2003 M_w 8.3 Tokachi-oki, Japan Earthquake

Kazuki Koketsu[1], Ken Hatayama[2], Takashi Furumura[1], Yasushi Ikegami[1,3], and Shinichi Akiyama[3]

INTRODUCTION

Although most seismic damage occurs within 10–20 km of an event, long-period waves can cause destruction at much greater distances. The long-period component of seismic ground motion generated by earthquakes attenuates more slowly with distance than higher frequencies and so persists to much greater ranges. Large-scale structures such as tall buildings and big tanks can resonate with the long-period ground motion because their own natural periods are in the same frequency band. The severity of shaking can be such that panic is produced for people in high-rise buildings from earthquakes several hundreds of kilometers away (Pan, 1995; Pan and Sun, 1996). Such long-period ground motions can even be damaging in some circumstances; the worst example occurred with more than 20,000 fatalities in Mexico City at a distance of 400 km from the 1985 Michoacán earthquake (Beck and Hall, 1986).

A further example was provided by Tomakomai, a coastal city on the island of Hokkaido in northern Japan, which was hit by long-period ground motion from the Tokachi-oki earthquake 250 km away on the morning of 26 September 2003 (local time = UT + 9 hours). This M_w 8.3 earthquake was the largest event in the world in 2003 (National Earthquake Information Center, 2004), but damage was not extensive because the location is offshore. No one was killed, although two people fishing during the tsunami are missing. We note that no intensities larger than 6– were observed on the JMA scale, where the highest ranks are 7 and 6+ (Japan Meteorological Agency, 2003). The intensity at Tomakomai was only 5–, which corresponds to no structural damage to houses. Many oil tanks were damaged by the long-period ground motions, however, and two of them caught fire (Coffin and Hirata, 2003), as shown in Figure 1. This article will discuss these damaging long-period ground motions and our preliminary analyses. The earthquake itself has been discussed in more detail in the special section of *Earth, Planets and Space* **56**(3) (*e.g.*, Koketsu *et al.*, 2004).

1. Earthquake Research Institute, University of Tokyo, Japan
2. National Research Institute of Fire and Disaster, Japan
3. CRC Solutions, Tokyo, Japan

OBSERVATIONS

Tomakomai is located in the center of the Yufutsu sedimentary basin facing the Pacific Ocean to the south (Figure 2). We are able to combine observations from the nationwide seismometer arrays K-NET (Kinoshita, 1998) and KiK-net (Aoi *et al.*, 2000) to characterize the nature of the ground motion. Within the sedimentary basin at stations HKD129 and IBUH05 there are very clear long-period components of ground motion with long duration. A shorter long-period wave train is also found at station HDKH04 near the eastern edge of the basin (Figures 3A and 3B). Particle motion analysis (Figure 3D) helps identify the changing nature of the wave trains. The initial short-period part of the seismogram at HDKH04 consists primarily of *S* waves, since the ground motion is polarized in the radial (east-west) direction from the earthquake source of low-angle reverse faulting. This is followed by a couple of cycles of waves with rather long periods, as indicated by the orange underbars in Figures 3A and 3B. These particle motions are also polarized in the radial direction, so they can be identified as surface Rayleigh waves. These waves can even be found at HDKH06 outside the basin, although they are contaminated by short-period reverberations. This means that these Rayleigh waves must have been generated in the source region or during their passage to HDKH06.

The second segment of long-period ground motion, indicated in purple in Figures 3A and 3B, is polarized in the transverse direction with oval orbits (Figure 3D). This portion of the seismograms consists mainly of surface Love waves and some other waves associated with the 3D complexity of the basin structure. The maximum ground velocity of the surface waves on the north-south seismograms is larger at station HKD129 in Tomakomai (32.6 cm/s) than at HDKH04 (30.4 cm/s), even though the latter station is 40 km closer to the earthquake. The duration of the long-period ground

▲ **Figure 1.** Aerial view of the fire in the oil tank damaged by long-period ground motions from the 2003 Tokachi-oki, Japan earthquake (courtesy of Dr. Hiroshi Koseki, National Research Institute of Fire and Disaster, Japan).

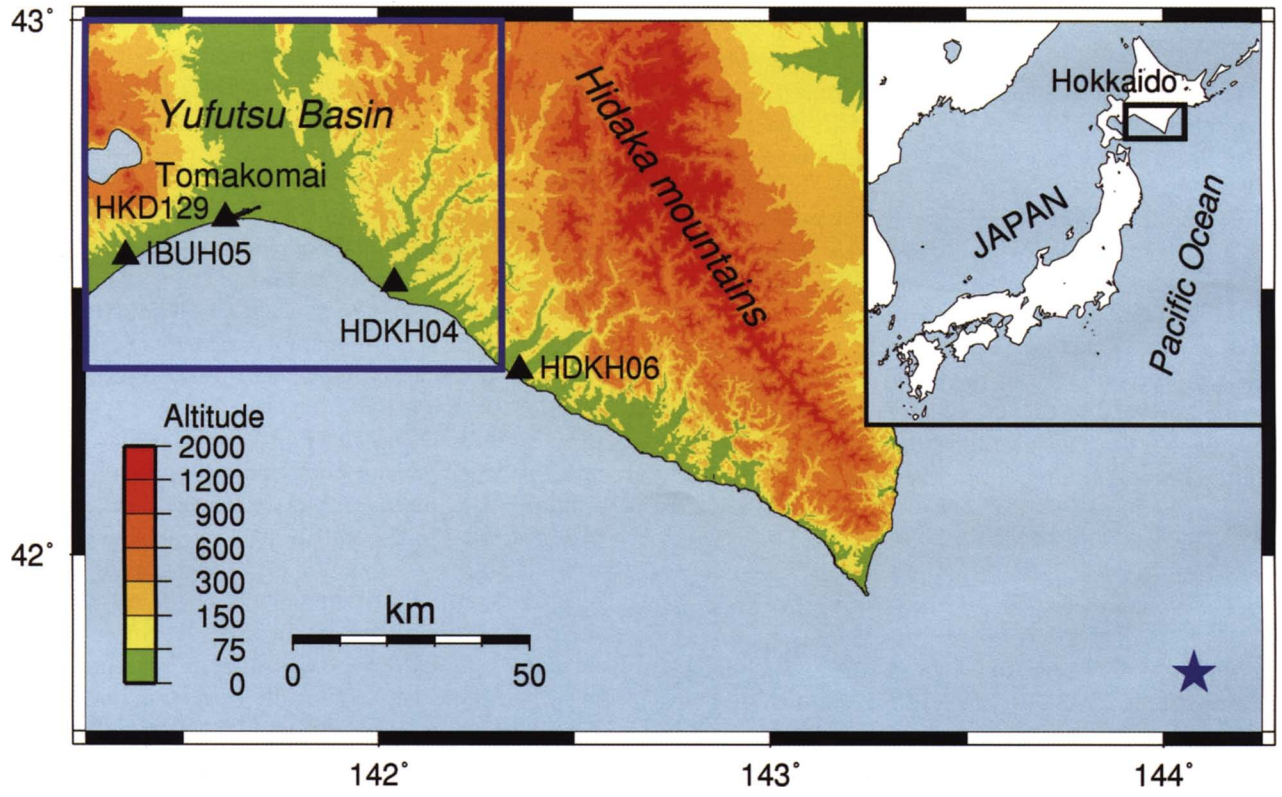

▲ **Figure 2.** Index map of the Tomakomai and Hidaka regions in Hokkaido, Japan. The black triangles denote seismometer stations in and around the Yufutsu basin, where strong ground motions from the 2003 Tokachi-oki earthquake were observed. The blue star indicates the epicenter of the earthquake.

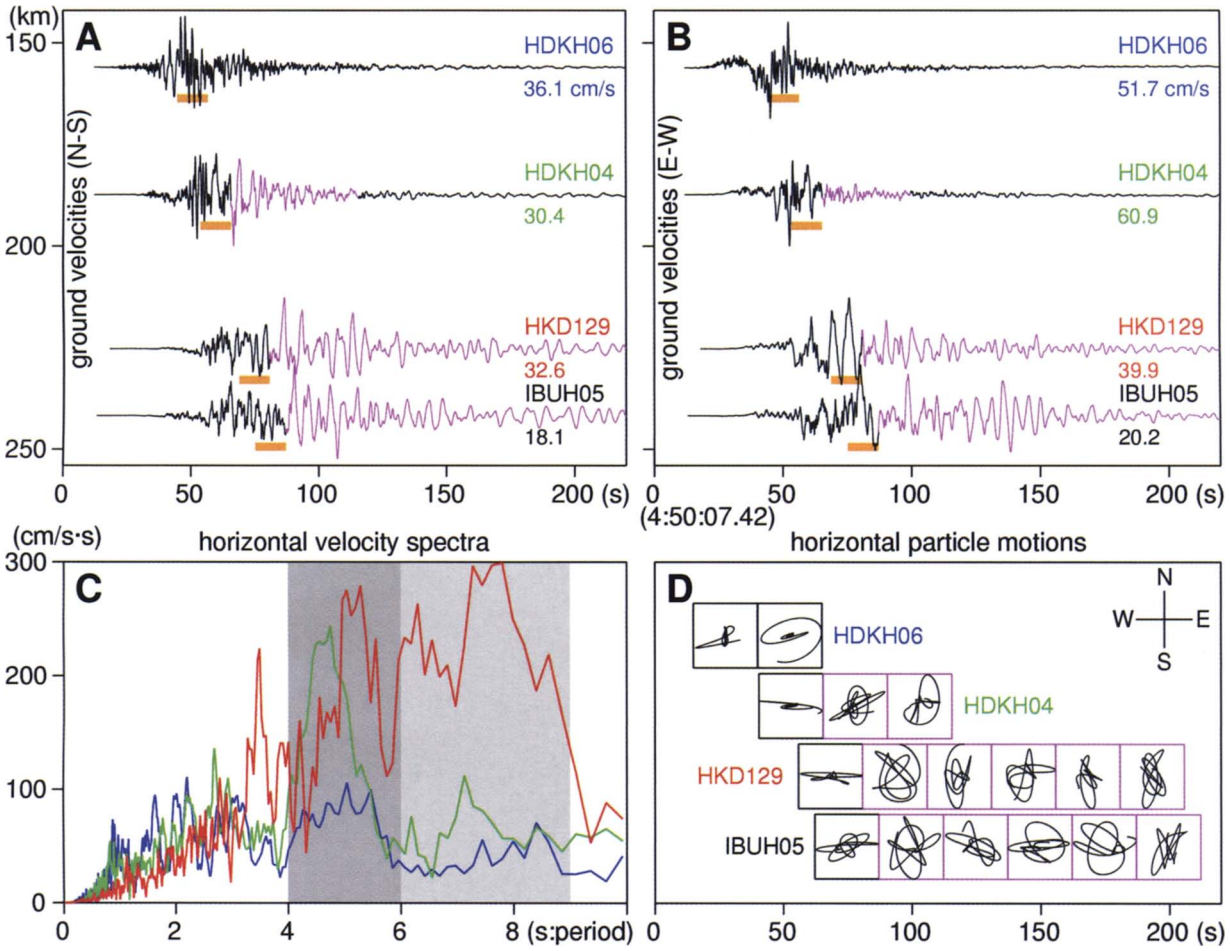

▲ **Figure 3.** Sections of (A) north-south and (B) east-west velocity seismograms observed at the four stations. The traces consist of *S* waves, Rayleigh waves (orange underbar), and induced Love waves (purple portion). Panels C and D display the velocity spectra and horizontal particle motions at HDKH06 (blue), HDKH04 (green), HKD129 (red), and IBUH05 (black).

motions is also longer at HKD129 by about 100 s. Similar behavior to HKD129 is seen at IBUH05, which is located on the other side of the Yufutsu basin.

The frequency spectrum of horizontal ground velocity at HKD129 is dominated by components in the period range from 4–9 s (red curve in Figure 3C), whereas the main contribution at HDKH04 lies in the 4–6 s band (green curve). Although the seismogram at HDKH06 shows no obvious long-period arrivals, we can find modest peaks with these periods in the ground velocity spectra observed there (blue curve). The high-amplitude peaks correspond to the Rayleigh waves, which travel via HDKH06 to the basin edge near HDKH04 and are then converted to basin surface waves with similar or longer periods (Kudo, 1980; Koketsu and Kikuchi, 2000). The Love waves with periods from 6–9 s are produced at the edge of the basin and develop further as they propagate across the basin (Frankel *et al.*, 1991; Hatayama *et al.*, 1995; Frankel *et al.*, 2001). The basin surface waves create the 4–6 s peak in the spectrum at HDKH04, which extends after further propagation to HKD129 into the much broader zone shown in light gray in Figure 3C.

SIMULATIONS

The above interpretations are supported by preliminary 3D numerical simulations of the ground motion. A 3D structural model for the region outlined in blue in Figure 2 was constructed exploiting the results of reflection and microtremor surveys (Asano *et al.*, 1989), together with the surface and seabed topography (Geographical Survey Institute, 2004; Japan Oceanographic Data Center, 2004). The sea to the south of the Yufutsu basin was included in the model with zero rigidity (Stephen, 1988). The ground-motion simulations were then carried out using a finite-element method with a voxel mesh (Koketsu *et al.*, 2004) and excitation by an input plane wave specified by the seismic motion observed in the borehole site at HDKH06, located just outside the region. To account for amplification at the free surface, the borehole motion amplitude was reduced by one half.

The pattern of horizontal ground motion from the numerical simulations is shown in Figure 4, superimposed on the surface topography. The first snapshot at 4:51:17.52 (70.10 s after the earthquake origin time of 4:50:07.42) shows the moment when the *S* waves emerge into the central part of the

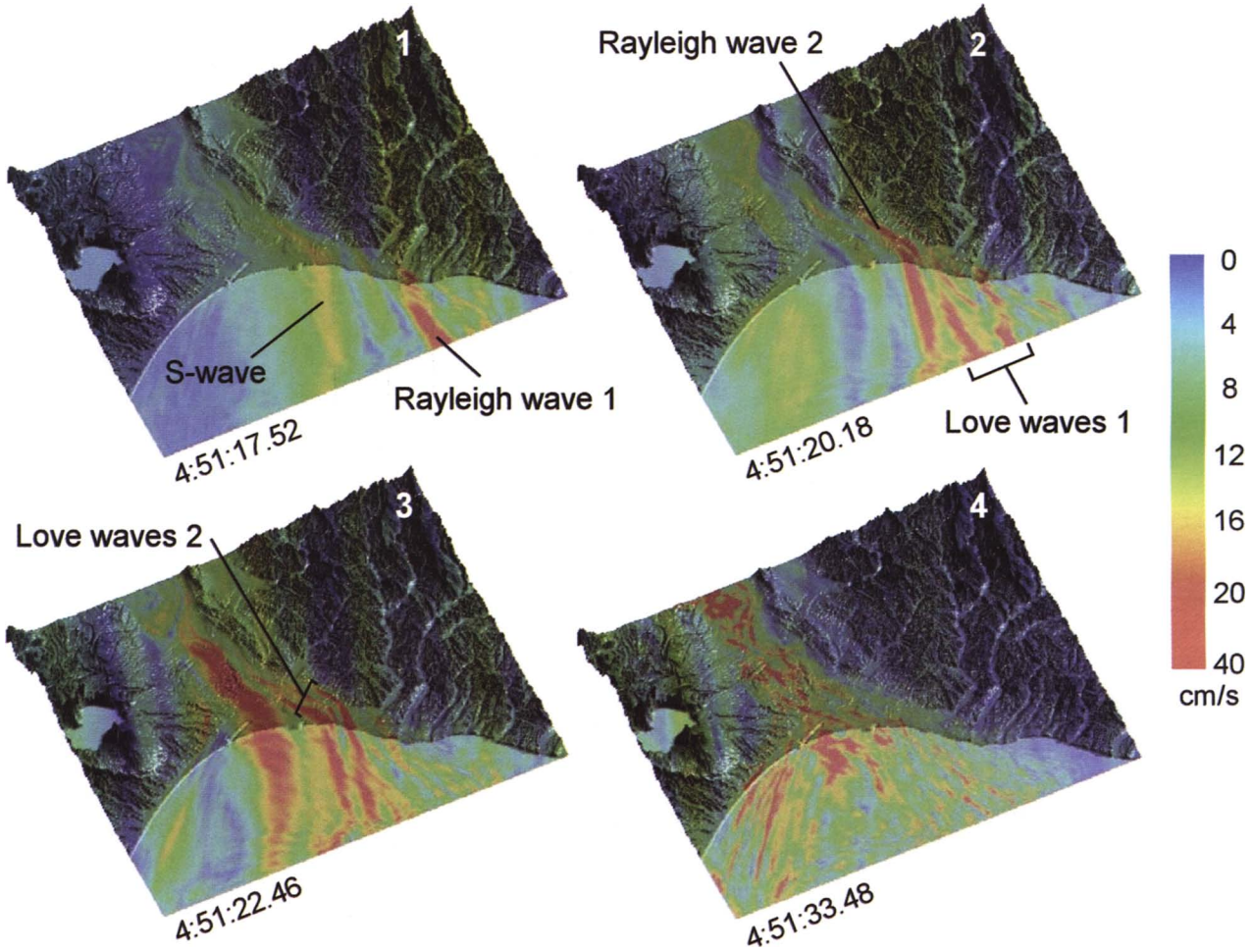

▲ **Figure 4.** Snapshots of the distribution of simulated horizontal ground velocities (1–4). The significant wavefronts are specified with the labels "S-wave", "Rayleigh waves 1 & 2", and "Love waves 1 & 2."

basin. In this frame, the Rayleigh wave from the source region is converted to a basin surface wave at the eastern basin edge, which lies under the sea. Another basin surface wave is converted along the boundary between the basin and the Hidaka Mountains ("Rayleigh wave 2" in frame 2 at 4:51:20.18). These two Rayleigh waves collide at the southern coast of the Yufutsu basin and form a large-amplitude disturbance with an angular margin as can be seen in the third snapshot at 4:51:22.46. Both of the Rayleigh waves contributed to the wavefront at the cusp near the coast, close to Tomakomai, so that the east-west component at HKD129 shows well developed long-period ground motions, as indicated by the orange underbar in Figure 3B.

We can identify short-period arrivals behind the *S* and Rayleigh waves in the HDKH06 seismograms (Figures 3A and 3B). This *S* coda hits the basin edge and produces the basin Love waves. The first Love wave train is produced at the undersea part of the basin edge as shown in snapshot 2. In a similar fashion to the converted Rayleigh wave in the basin, the second Love wave train was produced at the basin-mountain boundary ("Love waves 2" in snapshot 3). The two Love waves interact with each other, and new Rayleigh waves can be generated from interconversions of surface-wave modes in the 3D basin structure. The combination of all these processes results in whole-basin reverberation with long-period ground motion, as shown in snapshot 4, which matches the behavior seen on the HKD129 and IBUH05 seismograms in Figures 3A and 3B.

The second Love wave train can be confirmed by the observed particle motions. Figure 5 displays the snapshot for the period from 70–80 s after the origin time. The motions at stations IBUH03 and ATSUMA near the basin-mountain boundary are polarized in the northwest-southeast direction, whereas the orbit at station HKD126 shows only the transverse motion of the ordinary Love wave. We conducted a temporary array observation of the aftershocks in October 2003. Its result also shows particle motions polarized in the direction along the boundary between the Yufutsu basin and the Hidaka Mountains.

OIL TANKS

The strong long-period ground motion can have destructive impact on large structures whose natural periods lie in the

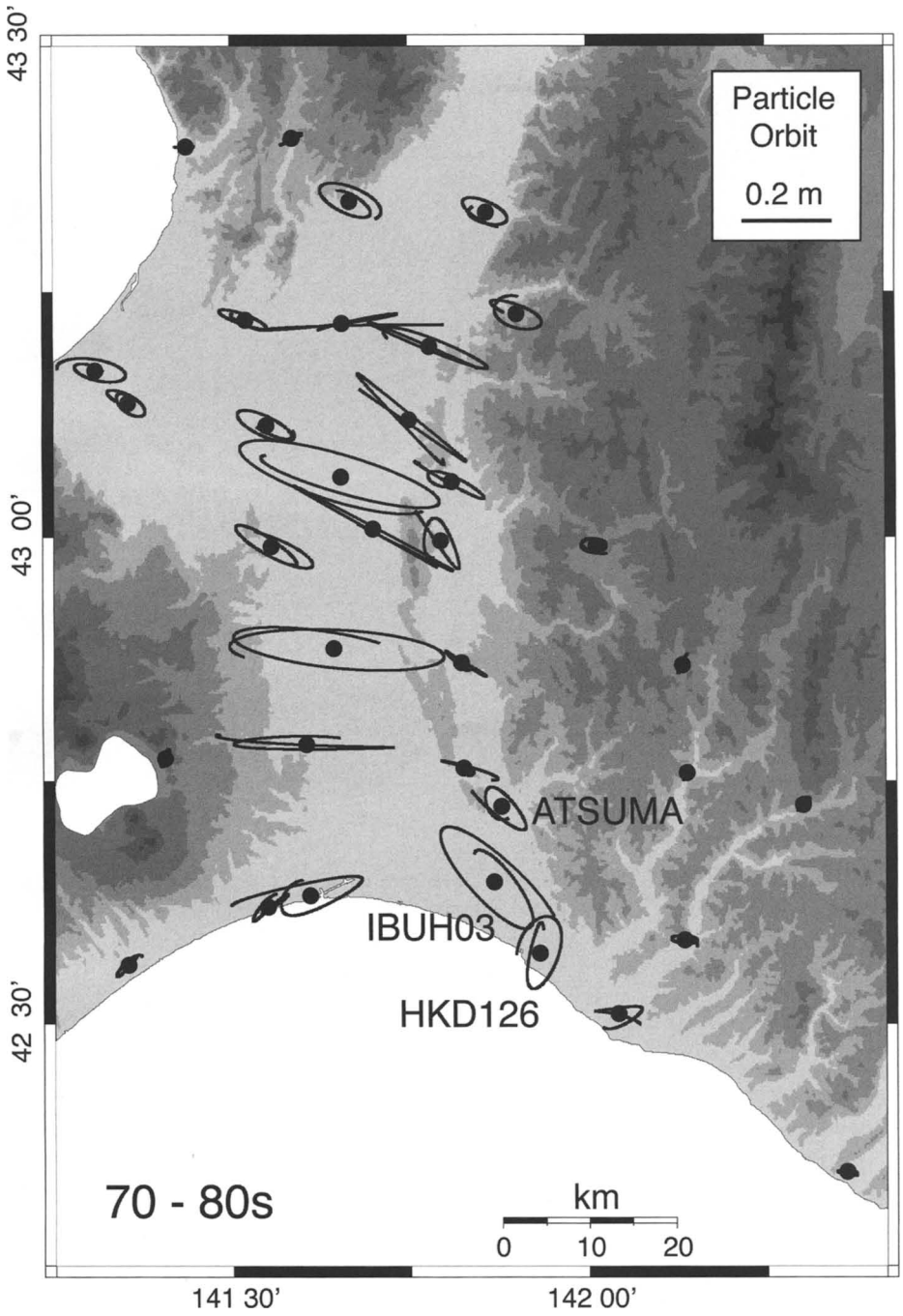

▲ **Figure 5.** Distribution of particle orbits of the long-period ground motions in the Yufutsu basin and its extensions during the period from 70–80 s after the earthquake. The motions polarized in the direction along the basin-mountain boundary were observed at stations IBUH03 and ATSUMA.

same period band. In the case of Tomakomai, a number of oil tanks were damaged. We use the recorded ground motion to investigate the behavior of an oil tank that was damaged during the earthquake and caught fire two days later (Figure 6A and Figure 1), by using finite-element analysis of fluid sloshing with solid voxels and fan-shaped liquid elements (Figure 6B). The tank had a capacity of about 30,000 m^3 and at the time of the earthquake contained 25,000 m^3 of volatile chemicals called naphtha (Hatayama *et al.*, 2004). The first step was to solve for the eigen periods of vibration of the tank; the period 7.12 s for the fundamental mode of the sloshing lies in the middle of the period band for the large-amplitude ground motion at Tomakomai (red spectrum in Figure 3C). The naphtha in the tank would therefore resonate with the ground motion, producing large sloshing waves.

The second step was to extend to a full dynamic analysis with a fixed foundation subject to the ground motion observed at station HKD129, located very close to the tank

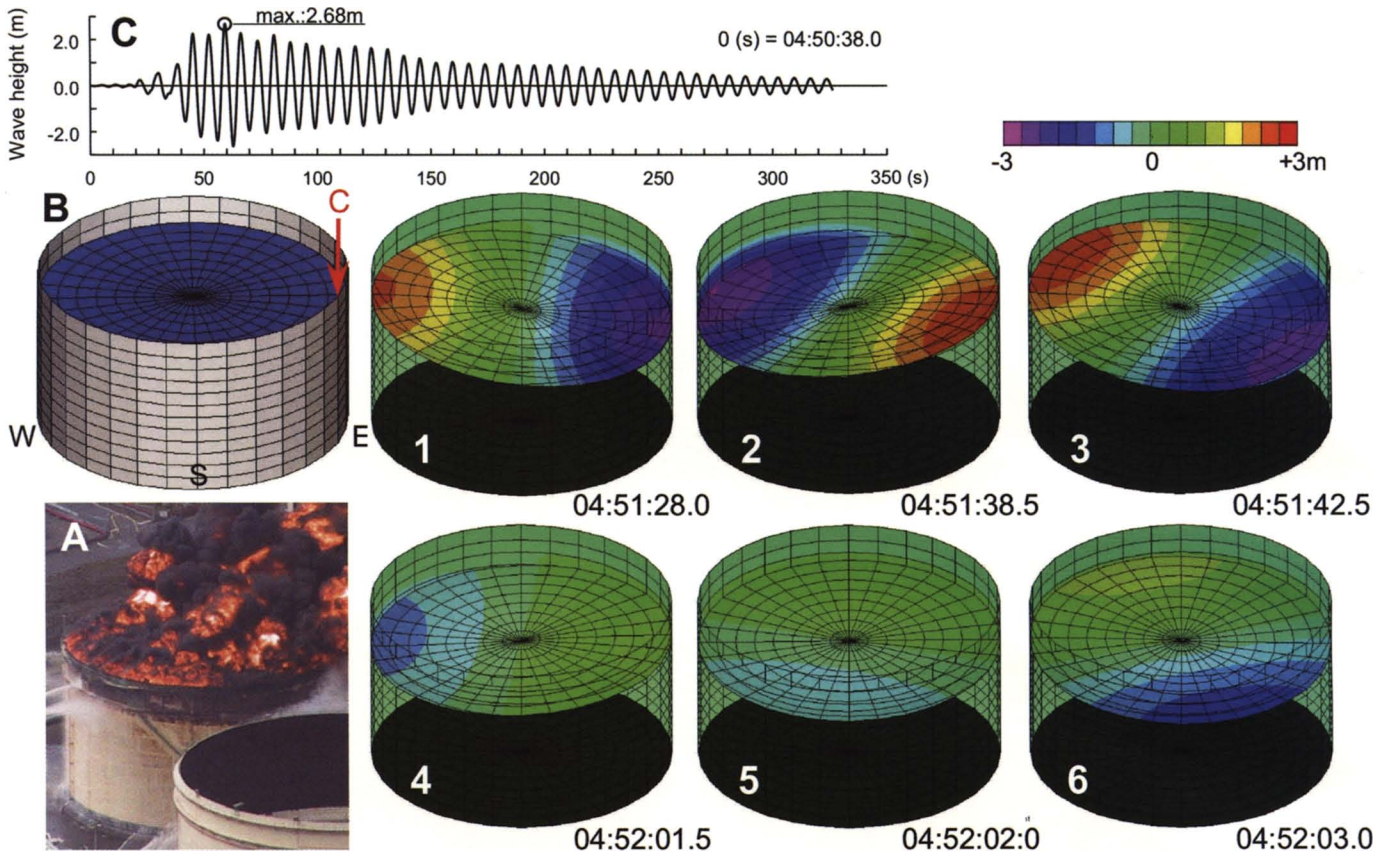

▲ **Figure 6.** Snapshots of the distribution of simulated naphtha surface motions (1–6). Panels A and B show a photo of the fire in the tank and an FEM model of the tank, respectively. The red arrow points to the position of the highest sloshing wave. Panel C displays the time history of the sloshing at this position.

(Figures 3A and 3B). The computed surface motion for the naphtha is displayed in Figures 6-1 to 6-6. The arrival of the basin Rayleigh waves provides the first long-period impact on the tank. Since this wave is polarized in the east-west direction, the naphtha initially vibrated along this direction, as shown in snapshot 1. The second impact was then generated by the basin Love waves, which were mostly polarized in the north-south direction. The initial east-west sloshing decayed rather slowly, however, and the ground motion excited by the Love waves included some east-west motions arising from the 3D basin structure. Accordingly, snapshots 2 and 3 show a northwest-southeast motion of the naphtha surface.

The sloshing motion builds up to an amplitude of 2.68 m around the time of snapshot 3. Position C of the maximum height reached is shown with the red arrow in Figure 6B. The long-period ground motion continued for more than two minutes after the highest sloshing, with a counterclockwise rotation as shown in the particle motion diagram of Figure 3D. Consequently, the motion on the naphtha surface was also rotated counterclockwise, as shown in snapshots 4 to 6. Figure 6C shows the time history of the sloshing wave height at point C. Since the damping factor of the naphtha is as small as 1%, the wave height decreased very slowly and large sloshing continued for a long time.

CONCLUSIONS

In September 2003 the city of Tomakomai in Hokkaido, Japan suffered substantial damage to large oil tanks from long-period seismic waves generated by the 2003 Tokachi-oki earthquake, more than 250 km away offshore. The disturbance in the large sedimentary basin within which the city lies is characterized by combining observations and 3D numerical simulations. A very important contribution came from surface waves stimulated in the basin, either directly or by conversion at the margins, which led to large amplitudes and duration of shaking. Fluid sloshing in a damaged oil tank occurred with a period close to that of the dominant ground motion, producing meters of displacement and a long fluid oscillation that contributed to the destruction of a floating roof. The naphtha was then exposed to the air and became flammable. An unknown cause finally ignited the subsequent fires.

The 2003 Tokachi-oki, Japan earthquake reproduced the phenomenon of damage at a distance seen in the 1985 Michoacán earthquake and demonstrates that a magnitude 8 earthquake can generate damaging long-period ground motions in a distant sedimentary basin. Since no tall buildings were in Tomakomai, the tragedy in Mexico City was

fortunately not fully reproduced. The event does provide a timely reminder of the long-range impact of earthquake damage, however. A future San Francisco earthquake will cause not only tragedy in the Bay Area but might also have a severe impact on the deep sedimentary basin underlying Los Angeles. Heaton *et al.* (1995) have already warned us that a large earthquake just beneath a metropolitan area can severely damage structures with long natural periods. Distant earthquakes with magnitudes 8 and above are also potentially damaging for these structures.

ACKNOWLEDGMENTS

We thank Prof. Brian Kennett (ANU) and Dr. Susan Hough (USGS) for careful reviews. The National Research Institute of Earth Science and Disaster Prevention and JMA provided us with the strong-motion records. This study was supported by the Special Coordination Funds for Promoting Science and Technology, and the Special Project for Earthquake Disaster Mitigation in Urban Areas from MEXT of Japan.

REFERENCES

Aoi, S., K. Obara, S. Hori, K. Kasahara, and Y. Okada (2000). New strong-motion observation network: KiK-net, *Eos, Transactions of the American Geophysical Union* **81**, Fall Meeting Supplement, S71A-05.

Asano, S. (1989). *Study on a Deep Underground Structure for Accurate Ground Motion Prediction*, Grant-in-Aid for Scientific Research No. A-63-3, 163 pp.

Beck, J. L. and J. F. Hall (1986). Factors contributing to the catastrophe in Mexico City during the earthquake of September 19, 1985, *Geophysical Research Letters* **13**, 593–596.

Coffin, M. and N. Hirata (2003). Large earthquake strikes Hokkaido, Japan, *Eos, Transactions of the American Geophysical Union* **84**, 442.

Frankel, A. D., D. Carver, E. Cranswick, T. Bice, R. Sell, and S. Hanson (2001). Observations of basin ground motions from a dense seismic array in San Jose, California, *Bulletin of the Seismological Society of America* **91**, 1–12.

Frankel, A. D., S. Hough, P. Friberg, and R. Busby (1991). Observations of Loma Prieta aftershocks from a dense seismic array in Sunnyvale, California, *Bulletin of the Seismological Society of America* **81**, 1,900–1,922.

Geographical Survey Institute (2004). CD-ROM Versions of Digital Maps, http://www.gsi.go.jp/MAP/CD-ROM/cdrom.htm.

Hatayama, K., K. Matsunami, T. Iwata, and K. Irikura (1995). Basin-induced Love waves in the eastern part of the Osaka Basin, *Journal of Physics of the Earth* **43**, 131–155.

Hatayama, K., S. Zama, H. Nishi, M. Yamada, Y. Hirokawa, and R. Inoue (2004). Long-period ground motion and damage to oil storage tanks due to the 2003 Tokachi-oki earthquake, *Zisin* (*Journal of the Seismological Society of Japan*) (in press).

Heaton, T. H., J. F. Hall, D. J. Wald, and M. W. Halling (1995). Response of high rise and base-isolated buildings to a hypothetical M_w 7.0 blind thrust earthquake, *Science* **267**, 206–211.

Japan Meteorological Agency (2003). Monitoring of Earthquakes and Volcanic Activities and Tsunami Forecasting, http://www.jma.go.jp/JMA_HP/jma/jma-eng/activities/seismo.html.

Japan Oceanographic Data Center (2004). J-DOSS: JODC Data Online Service System, http://www.jodc.go.jp/service.htm.

Kinoshita, S. (1998). Kyoshin Net (K-NET), *Seismological Research Letters* **69**, 309–332.

Koketsu, K., H. Fujiwara, and Y. Ikegami (2004). Finite-element simulation of seismic ground motion with a voxel mesh, *Pure and Applied Geophysics* **161**, 2,463–2,478.

Koketsu, K., K. Hikima, S. Miyazaki, and S. Ide (2004). Joint inversion of strong motion and geodetic data for the source process of the 2003 Tokachi-oki, Hokkaido, earthquake, *Earth, Planets and Space* **56**, 329–334.

Koketsu, K. and M. Kikuchi (2000). Propagation of seismic ground motion in the Kanto basin, Japan, *Science* **288**, 1,237–1,239.

Kudo, K. (1980). A study on the contribution of surface waves to strong ground motions, *Proceedings of the 7th World Conference of Earthquake Engineering* **2**, 499–506.

National Earthquake Information Center (2004). Significant Worldwide Earthquakes in 2003, http://wwwneic.cr.usgs.gov/neis/eq_depot/2003/index.html.

Pan, T.-C. (1995). When the doorbell rings: A case of building response to a long-distance earthquake, *Earthquake Engineering and Structural Dynamics* **24**, 1,343–1,353.

Pan, T.-C. and J. Sun (1996). Historical earthquakes felt in Singapore, *Bulletin of the Seismological Society of America* **86**, 1,173–1,178.

Stephen, R. A. (1988). A review of finite-difference methods for seismo-acoustics problems at the seafloor, *Review of Geophysics* **26**, 445–458.

Earthquake Research Institute
University of Tokyo
Japan
koketsu@eri.u-tokyo.ac.jp
(K.K., T.F., Y.I.)

National Research Institute of Fire and Disaster
Japan
(K.H.)

CRC Solutions
Tokyo
Japan
(Y.I., S.A.)